

56

## A NUMERICAL APPLICATION OF THE SLIP LINE FIELD METHOD TO EXTRUSION THROUGH CONICAL DIES

J. L. CHENOT, L. FELGERES†, B. LAVARENNE and J. SALENÇON‡

CEMEF, Ecole des Mines de Paris, Zac de Sophia-Antipolis, B. P. No. 1. 06560 Valbonne, France

(Communicated by B. NAYROLES)

**Abstract**—The industrial importance of cold extrusion is now well known. Unfortunately, the productivity of the process is restricted by the manifestation of a specific defect: the central burst, which is closely linked to ductility and to a depressive stress state in the core of material. An accurate knowledge of these facts is therefore necessary to the extension of the process. In this paper, we develop a slip line field model in order to calculate exactly the hydrostatic pressure on the axis of the system. Its peculiarity is that it can be associated with a mechanical test of material ductility. This method is developed for axisymmetric extrusion through conical dies, with a perfectly plastic material, obeying Tresca's yield criterion with its associated flow rule and with the Haar-Kärman hypothesis. We assume that the pressure has a linear distribution along the die, which makes it possible to construct the slip line field. We then derive the velocity field, and determine by trial and error the pressure gradient along the die so that the velocity field satisfies all the boundary conditions. We apply this method to several extrusion ratios and die-angles; we compute the stress field in the deformed regions, obtaining an upper-bound for the extrusion pressure and a value for the hydrostatic pressure on the axis. Comparisons with experimental results show quite a good agreement between theoretical and experimental values of the extrusion pressure. The method will enable us in a future work to introduce friction along the die, metal work hardening and different profiles of the die.

### INTRODUCTION

EXTRUSION through conical dies, with the apparition of defects such as central burst, has been studied by several authors [1-3]. B. Avitzur [1] has given a criterion for central burst, by an upper bound approach. However, it appears that the knowledge of the stress field, in particular of the hydrostatic pressure in the vicinity of the axis, could be of great help in such a study, since it would make it possible to take the ductility of the material into account. It is obvious then that the slip line field method must be used.

The basic equations for an axially symmetric plastic flow are given by Hill [4]. For Tresca's material under the Haar-Kärman hypothesis, punch indentation problems were investigated by Shield [5], Eason and Shield [6] and Spencer [7]; Szczepinski *et al.* [8] dealt with the plastic flow of bars under tension. Murota [9] gave a first analysis of axisymmetric extrusion, but had not solved the problem of an exact calculation on the axis.

In this paper, the classical slip line equations are used, under the assumption of a rigid perfectly plastic material which obeys Tresca's yield criterion with its associated flow rule; we make the Haar-Kärman hypothesis.

Incremental arcs of slip lines are treated during the integration as arcs of circles; this gives a great accuracy in calculations and removes the indetermination of terms ( $dr/r$ ) on the axis of symmetry ( $r = 0$ ).

A detailed analysis of axially symmetric plastic flow for Tresca's material is given by Shield [5].

We just recall the basic equations in Part 1 of this paper. Part 2 will show the resolution, by means of a computer, of the final differential equations, yielding the slip line field with its associated stresses and compatible velocities. The program finally prints out the following results:

- Coordinates of the slip line field nodal points.
- Principal directions at the nodal points.
- Hydrostatic pressure at the nodal points.
- Velocities at the nodal points.
- Extrusion pressure.
- Pressure distribution on the die.

†L. Felgeres, Centre de Recherches Voreppe, Aluminium Pêchiney, BP 24, 38340, Voreppe.

‡J. Salençon, Laboratoire de Mécanique des Solides, 91128 Palaiseau Cedex, Ecole Nationale des Ponts et Chaussées, Paris.

It is only necessary to specify the die geometry and boundary conditions, the calculation being performed in an iterative manner.

In Part 3, we present the results obtained for different geometrical conditions and compare them to experiments on extrusion pressures made by Guimier [10] (Régie Nationale des Usinés Renault).

Part 4 is devoted to a critical analysis of the method and of the possibilities of further extending the model.

## 1. BASIC EQUATIONS

### 1.1 Notations

Using cylindrical coordinates  $(r, \theta, z)$ , the velocity components are denoted by:  $U_r, U_\theta, U_z$  (see Fig. 1).

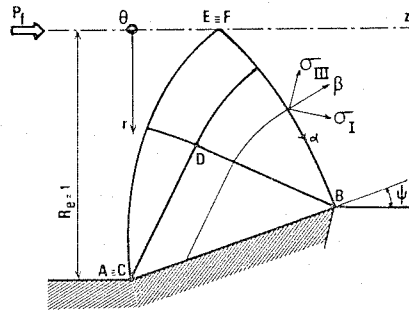


Fig. 1.

Due to the symmetry of the problem, and the material being assumed isotropic and homogeneous

$$U_r = U_r(r, z)$$

$$U_\theta = 0$$

$$U_z = U_z(r, z).$$

So the strain rate tensor is

$$\dot{\epsilon} = \begin{vmatrix} \frac{\partial U_r}{\partial r} & 0 & \gamma_{rz} \\ 0 & U_r/r & 0 \\ \gamma_{rz} & 0 & \frac{\partial U_z}{\partial z} \end{vmatrix}$$

where

$$\gamma_{rz} = \frac{1}{2} \left( \frac{\partial U_r}{\partial z} + \frac{\partial U_z}{\partial r} \right),$$

and  $\theta$  is therefore a principal direction for  $\dot{\epsilon}$ .

The stress tensor is  $\sigma$ . Its principal values are denoted by  $\sigma_1, \sigma_2, \sigma_3$ , with the convention  $\sigma_1 \geq \sigma_2 \geq \sigma_3$  (tensile stresses positive).

The material is assumed to obey Tresca's yield criterion

$$\sigma_1 - \sigma_3 \leq 2k = Y \quad (\text{yield stress})$$

with its associated flow rule.

Since we use the rigid plastic model, it follows that  $\theta$ , a principal direction for  $\dot{\epsilon}$  is also a principal direction for  $\sigma$ , wherever  $\dot{\epsilon} \neq 0$

$$\sigma = \begin{vmatrix} \sigma_r & 0 & \tau_{rz} \\ 0 & \sigma_\theta & 0 \\ \tau_{rz} & 0 & \sigma_z \end{vmatrix}$$

$\sigma_I$  and  $\sigma_{III}$  denoting the principal stresses in the  $(r, z)$  plane, we can define two parameters  $p$  and  $\phi$

$$p = -\frac{\sigma_r + \sigma_z}{2} = -\frac{\sigma_I + \sigma_{III}}{2} \quad (\dagger)$$

$$\phi = (r, \sigma_I) - \frac{\pi}{4} = (r, \alpha) \quad (\text{see Fig. 2})$$

where  $\sigma_I \geq \sigma_{III}$ .

### 1.2 Hypothesis and basic equations

The stress components satisfy the equations of equilibrium

$$\left. \begin{aligned} \frac{\partial \sigma_r}{\partial r} + \frac{\partial \tau_{rz}}{\partial z} + \frac{\sigma_r - \sigma_\theta}{r} &= 0 \\ \frac{\partial \tau_{rz}}{\partial r} + \frac{\partial \sigma_z}{\partial z} + \frac{\tau_{rz}}{r} &= 0 \end{aligned} \right\} \quad (1)$$

(body forces and inertial terms are negligible), and in the plastic regions, Tresca's yield criterion is reached

$$\sigma_1 - \sigma_3 = 2k = Y.$$

But the problem cannot be solved without another relation (since we have four unknowns  $\sigma_r, \sigma_\theta, \sigma_z, \tau_{rz}$ ).

The Haar-Kärman hypothesis states that in the plastic regions,  $\sigma_\theta = \sigma_2 \ddagger$  and is equal either to  $\sigma_1$  or to  $\sigma_3$ : on Tresca's hexagone, the stress state is represented by points A or F (see Fig. 3).

This hypothesis fits in with the form assumed for the velocity field where  $U_\theta = 0$  (see Salençon[11]).

Since we have, in the case of extrusion,  $U_r < 0$ , it follows that

$$\dot{\epsilon}_2 = \dot{\epsilon}_\theta = \frac{U_r}{r} < 0,$$

the stress-state corresponds to point A and so

$$\left. \begin{aligned} \sigma_1 &= \sigma_2 + 2k \\ \sigma_3 &= \sigma_2 \quad (\S) \end{aligned} \right\} \quad (2)$$

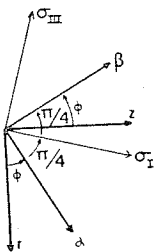


Fig. 2.

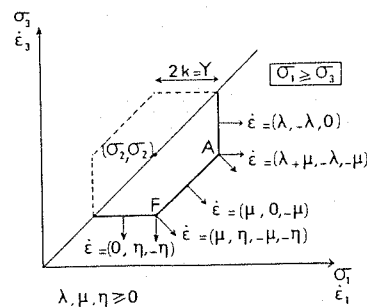


Fig. 3.

†Notice that the hydrostatic pressure  $P$  is equal to

$$P = -(\sigma_1 + \sigma_2 + \sigma_3)/3 = 2p/3 - \sigma_\theta/3.$$

‡The distinction between arabic and latin subscripts (1, 3) and (I, III) is, therefore, no longer to be made.

§The hydrostatic pressure  $P$  is now equal to

$$P = p + k/3.$$

The equations for the velocity field are derived from the flow rule and can be written as

Incompressibility of the material:

$$\frac{\partial U_r}{\partial r} + \frac{U}{r} + \frac{\partial U_z}{\partial z} = 0.$$

Isotropy of the material

$$\frac{\partial U_r / \partial z + \partial U_z / \partial r}{\partial U_r / \partial r - \partial U_z / \partial z} = -\cot 2\phi.$$

(3)

Positivity of the two parameters  $\lambda$  and  $\mu$  which define the strain-rate (see Fig. 3)

$$\lambda \geq 0$$

$$\mu \geq 0.$$

### 1.3 Final equations

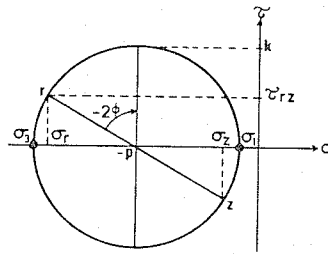


Fig. 4.

The stress state can be represented on Mohr's circle (in the  $(\sigma, \tau)$  plane) as shown in Fig. 4. The stress components can then be written

$$\left. \begin{aligned} \sigma_r &= -p - k \sin 2\phi \\ \sigma_z &= -p + k \sin 2\phi \\ \sigma_\theta &= -p - k \\ \tau_{rz} &= k \cos 2\phi. \end{aligned} \right\} \quad (4)$$

By substituting relations (4) into eqns (1), we get a hyperbolic system for the two functions  $p$  and  $\phi$  in the two variables  $r$  and  $z$ . The characteristics are found to be  $\alpha$ - and  $\beta$ - lines and the following differential equations are satisfied

$$\left. \begin{aligned} dp + 2kd\phi - \frac{k}{r}(dr - dz) &= 0 \quad \text{on an } \alpha\text{-line} \\ dp - 2kd\phi - \frac{k}{r}(dr + dz) &= 0 \quad \text{on a } \beta\text{-line.} \end{aligned} \right\} \quad (5)$$

The system of eqns (3) is also hyperbolic for the two functions  $U_r$  and  $U_z$ , with the same characteristics, and can take the form

$$\left. \begin{aligned} dU - Wd\phi + \frac{1}{2r}(Udr - Wdz) &= 0 \quad \text{on an } \alpha\text{-line} \\ dW + Ud\phi + \frac{1}{2r}(Udz + Wdr) &= 0 \quad \text{on a } \beta\text{-line} \end{aligned} \right\} \quad (6)$$

where  $U$  and  $W$  are the velocity components along  $\alpha$ - and  $\beta$ - lines.

The positivity conditions for parameters  $\lambda$  and  $\mu$  imply

$$\Gamma = \frac{\partial U}{\partial s_\beta} + \frac{\partial W}{\partial s_\alpha} + U \frac{\partial \phi}{\partial s_\alpha} - W \frac{\partial \phi}{\partial s_\beta} \geq -\frac{U_r}{r} \geq 0. \quad (7)$$

1.4 Boundary conditions

1.4.1. *On the axis.* The stress state takes the form:

$$\phi = \pi/4 \quad \sigma_r = \sigma_\theta \quad \sigma_z = \sigma_1 \text{ (greatest principal stress)}$$

Two cases are possible:

First, conditions on  $AB$  make it possible to determine a field which reaches the  $z$ -axis at point  $F$  (Fig. 1);  $F$  is the only point of the plastic zone on the axis, and a special procedure is used to solve system (5), which is indeterminate for  $r = 0$ .

When the extrusion ratio increases, the plastically deformed region on the  $z$ -axis no longer reduces to point  $E$ : the slip line field is then bounded by the  $\alpha$ -line  $BE$  and the  $\beta$ -line  $AF$  (Fig. 5).

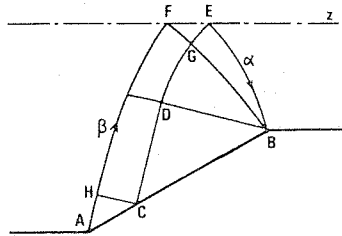


Fig. 5.

So we can construct the slip line field in regions EFG, FGCH and HCA.

1.4.2. *On the die.* Conditions concerning the stress field are: an arbitrary linear distribution of  $p$  is assumed on the die, of the form

$$p = p_0 + \frac{x}{l}(p(A) - p_0)$$

where  $p_0$  is the value of  $p$  at point  $B$ ,  $l$  the length  $BA$  of the die and  $x$  the abscissa along the die with  $B$  as an origin.

A coefficient of friction can be introduced, as will be shown below (Section 2.1).

1.4.3. *On the boundaries of the slip line field.* We denote by  $df_z$  the  $z$  component of the force acting on the cylindrical element of surface  $2\pi r dr$ . The value of  $p_0$  will be calculated from the condition

$$\int_{BE} df_z = 0$$

since there is no traction on the rod at the exit.

The extrusion force is given by

$$\int_{AF} df_z = F_{\text{extrusion}}$$

No velocity discontinuity is admissible on the two boundaries  $AF$  and  $BE$ , as indicated by Shield[5]; the result can easily be obtained by looking at the propagation equation for the velocity jump derived from (6). So the velocities on  $AF$  and  $BE$  are respectively

$$V_{\text{entry}}$$

and

$$V_{\text{exit}} = (1 - R) V_{\text{entry}} \text{ where } R_{\text{ratio}} \text{ is the reduction}$$

1.5 Iterative procedure

We assume an arbitrary slope  $[p(A) - p(B)]/l$  for a first calculation of the stress and the velocity field. The program then improves the value of this slope by a bisection type method until the velocity component normal to the die, denoted by  $V_n$ , becomes negligible.

2. COMPUTATION

2.1 Initiation

The slip line field is constructed starting from the boundary conditions on the die, where  $p$  is fixed as indicated in 1.4 and 1.5, and  $\phi$  depends on the friction coefficient: the angle formed by the normal to the die and principal direction ( $\sigma_1$ ) is  $\delta$  (Fig. 6b) so that the shear stress on the die is  $\bar{m}k$  (Tresca's friction) (Fig. 6a); that implies

$$\delta = \frac{1}{2} \text{Arc sin } \bar{m}, \text{ and so}$$

$$\phi_{AB} = \psi + \frac{\pi}{4} + \frac{1}{2} \text{Arc sin } \bar{m} \text{ (Fig. 6b).}$$

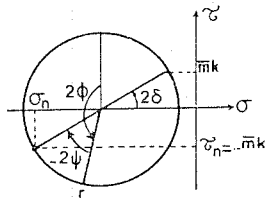


Fig. 6(a).

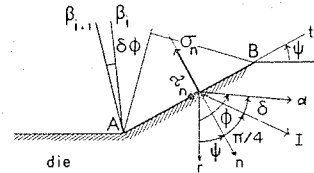


Fig. 6(b).

The points  $A$  and  $B$  are Prandtl's singularities and their  $\phi$ -parameter is a function of the  $-\alpha$  or  $-\beta$  line considered (Fig. 6b); in the computation, they are initiated by an angle increment

$$\phi(A_1) = \phi(A) + \delta\phi$$

$$\phi(A_2) = \phi(A) + 2\delta\phi$$

and so on; at each fictitious point  $A_i$  corresponds a different  $p$ -parameter deduced from eqn (1.5), for  $AA_i$  is a degenerated  $\alpha$ -line

$$[p(A_i) - p(A)] + 2[\phi(A_i) - \phi(A)] = 0.$$

Equivalent equations may be written for points  $B_j$ , which form a degenerated  $\beta$ -line.

2.2 Integration

2.2.1. *Calculations.* The approximate slip line field is generated by a mesh starting from the die surface: from the two diagonal points  $M_1$  and  $M_2$  of the mesh, point  $M$  is calculated as shown in Fig. 7.

Arcs  $MM_1$  and  $MM_2$  are treated as if they were arcs of circles; this makes the integration very accurate as shown in Appendix 1.

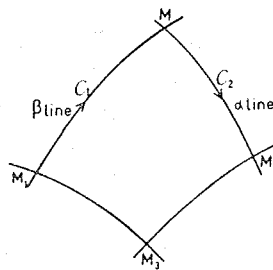


Fig. 7.

2.2.2. *Z-axis.* The accurate calculation of a point on the *z*-axis can be described as follows (see Fig. 8 and Appendix 2).

A test on  $\phi$  determines a point *R* near the *z*-axis where the angle  $\phi$  approaches  $(\pi/4)$ .

*QS* and *SR* are  $\alpha$  (respectively  $\beta$ ) slip lines along which  $E_1$  (respectively  $E_2$ ) are associated with the interpolation parameter  $\eta$  (respectively  $\zeta$ ).

*E* (respectively  $E'$ ) is the point on the axis corresponding to the  $\beta$ -line issued from  $E_1$  (respectively the  $\alpha$ -line issued from  $E_2$ ).

$\eta$  and  $\zeta$  are adjusted so that *E* and  $E'$  first have  $\phi$  parameters equal to  $\pi/4$ , and second  $E \equiv E'$ .

The approximation by circles also removes the indetermination of terms like  $(dr + dz)/r$  when integrating system (5) along the slip lines for  $r = 0$ .

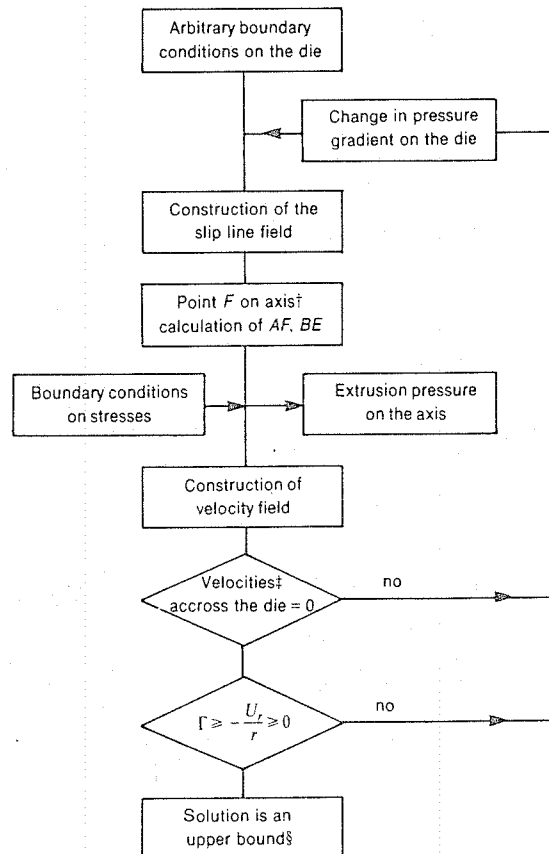
Lines *CE* and *BE* can then be calculated.

2.2.3. *Velocity fields.* The velocity components are derived from system (6), by means of a first order integration. Then, as said in (Section 1.5), the condition assumed on the die will be checked.

Finally, the velocity field will be admissible if conditions (7) are satisfied.

### 2.3. Programming

The general scheme is given below:



† Different die geometries were studied, for which it always occurred that  $E \equiv F$  was the only point of the deformed region on the *z*-axis.

‡ Test on velocities is

$$\int_{\text{die}} |V_n| dx \approx 0.$$

§ As the stressfield has not been constructed in the whole body, the solution is to be considered only as an upper-bound. However, as is often done, the heuristic assumption is made that the stress field so obtained in the plastically deformed zone is significant.

Our present program gives the final results in 50 seconds on a UNIVAC 1110 computer, for given die geometry and friction condition.

### 3. RESULTS

In Fig. 9 we show an example of a computed slip line field for a 30% area reduction, and with the die geometry:  $\psi = 20^\circ$ . Angle increments at  $A$  and  $B$  are  $\delta\phi = 1.5^\circ$ . The pressure drop along the die is:  $p(A) - p(B) = 0,25 Y$ .

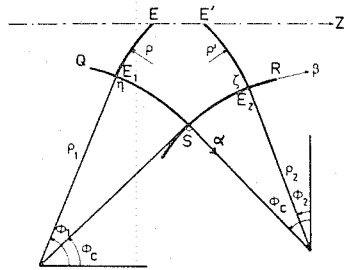


Fig. 8.

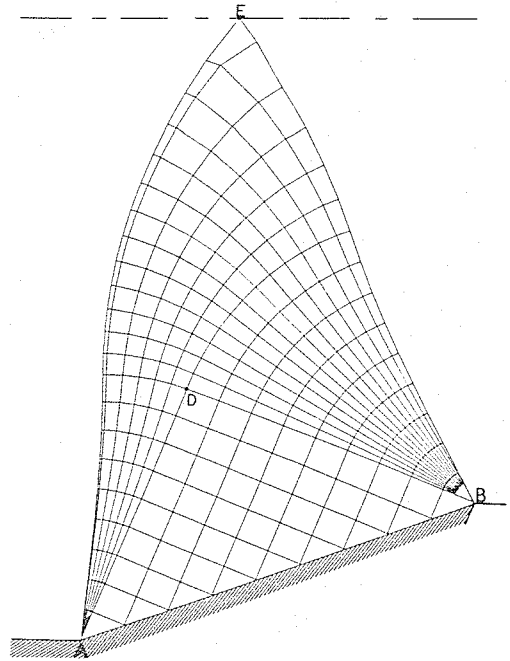


Fig. 9.

The great importance of arriving exactly on the axis is shown by the following results on points  $Q, R, S, E$  (Fig. 8):  $p(Q)/Y = P(R)/Y = -0.591$ ;  $p(S)/Y = -0.495$  and  $p(E)/Y = -0.815$ , where  $r_Q = 0.060$ ,  $r_R = 0.068$ ;  $r_S = 0.114$  and  $r_E = 0$  (reference  $r_A = R_{\text{entry}} = 1$ ). The calculated summation on normal die velocities is less than  $6 \cdot 10^{-4}$ .

Experimental results on extrusion forces were given by the work of Guimier *et al.* at the REGIE RENAULT [10]. Although the friction coefficient is not easy to determine experimentally (and taken equal to zero in our calculation), the results are in fairly good agreement. The value of the yield stress  $Y$  has been averaged in the form

$$Y = \lambda \frac{(\bar{\epsilon})^n}{n+1} \quad (10)$$

where a traction test determines the quantities  $\lambda$  and  $n$ .

The total equivalent strain  $\bar{\epsilon}$  has been averaged in the form

$$\bar{\epsilon} = \log(1 - R)$$

( $R$ : reduction ratio)

The Table 1 gives

1. Calculated results  $P_f/Y$  (extrusion force per unit area).
2. Experimental extrusion force  $F$  ( $\times 10^4 N$ ).
3.  $F/A_0 Y$ , ( $A_0$ : initial area;  $Y$ : average yield stress).

The slight discrepancies observed may result from the hypothesis of a perfectly plastic metal, the yield stress of which is assumed constant throughout the section. Moreover, it is to



TABLE 1

Geometry		$P_F/Y$	$\gamma=10^9 \text{Pa}$		$\gamma=5 \cdot 10^8 \text{Pa}$		$\gamma=8 \cdot 10^8 \text{Pa}$	
R	$\psi$		F	$F/A_0 Y$	F	$F/A_0 Y$	F	$F/A_0 Y$
20 %	10°	0.3	36.5	0.35	21.5	0.33	33.5	0.37
40 %	20°	.63	67.5	.63	57.5	.72	64.5	.62
40 %	30°	.76	70	.65	58	.73	64	.62
40 %	45°	.94	71	.66	65.5	.82	73.5	.71
60 %	30°	1.1			103	1.11	118.5	1.05
60 %	45°	1.3	139	1.27	122	1.32	136.	1.21

be noticed that the extrusion force is not constant during the forging process, and an average value is taken into account (Fig. 10[10]).

It must be also recalled that the calculation was performed assuming perfectly smooth dies.

The model has also been tested by means of incremental viscoplasticity experiments: rods are deformed in a first extrusion and circular grids are etched on two half-rods, on which an incremental deformation is made; this makes it possible to draw the slip lines directly [12]. This method shows a good qualitative agreement with our results and gives some information on the friction law, but its quantitative exploitation remains difficult.

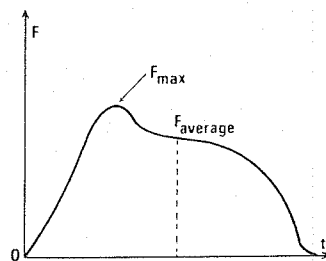


Fig. 10.

#### 4. DISCUSSION

As said above, the problem of strain-hardening may be of great importance, particularly in annealed materials. On pre-hardened materials, on the other hand, the yield stress probably varies throughout the section of the body and this is one more error factor. The model should be improved by taking into account the heterogeneity of the initial yield-stress; moreover, a first calculation performed under the non-hardening hypothesis gives an approximation of the strain-rate field in the plastic zone; during a second iteration, the integration can be carried out along the flow lines to introduce a strain-hardening law:  $Y = g(\bar{\epsilon})$ , where  $\bar{\epsilon}$  is the total equivalent strain.

Industrial applications of this work may be of great interest: as mentioned above, the first one was to establish a criterion for central burst, taking the ductility of the material into account, by means of an accurate knowledge of the internal stress state. Also, the method makes it possible to test different die contours, and to predict which one optimizes the extrusion pressure or favors the occurrence of defects.

The knowledge of the stress fields in a plastified zone may also lead to a first prediction of the residual stress field in the worked material, and of its metallurgical state.

*Acknowledgment*—The authors would like to thank the REGIE RENAULT for its financial support and for the leave to use its experimental results, which serve us as reference for the calculated ones.

\* coordinates of point  $E'$

$$r' = 0$$

$$z' = z_2 + \rho' \left( \cos \frac{\pi}{4} - \cos \phi_2 \right)$$

with

$$\rho' = \frac{r_2}{\sin \frac{\pi}{4} - \sin \phi_2}$$

\*The calculation of  $\rho'$  is made by integrating eqn (5.1), with a term

$$I_2 = \int_{E_2 E'} \frac{dz - dr}{r}$$

Along arc  $E_2 E'$

$$r = \rho' \left( \sin \frac{\pi}{4} - \sin \phi \right)$$

$$z = z' - \rho' \left( \cos \frac{\pi}{4} - \cos \phi \right)$$

so that

$$I_2 = \int_{\phi_2}^{\pi/4} \frac{\cos \phi - \sin \phi}{\sin \frac{\pi}{4} - \sin \phi} d\phi = \sqrt{2} \int_{\phi_2}^{\pi/4} \frac{\cos \left( \frac{\phi}{2} - \frac{\pi}{8} \right)}{\cos \left( \frac{\phi}{2} + \frac{\pi}{8} \right)} d\phi$$

that removes the indetermination for  $\phi = (\pi/4)$  and so

$$\rho' = p_2 - 2k \left( \frac{\pi}{4} - \phi_2 \right) - I_2$$

An analogous calculation can be made for point  $E$ , for a given value of  $\eta$ ;  $E_1$  is defined by

$$\phi_1 = \phi_Q - \eta(\phi_Q - \phi_S)$$

$\eta$  and  $\zeta$  are then optimized so that

$$z = z'$$

and

$$(p - p') \text{ minimum.}$$